

Showcasing research on protein crystallization in microdroplets using spontaneous emulsification from the group of Professor Akihide Hibara and Mao Fukuyama at the Department of Chemistry, Tokyo Institute of Technology, Japan.

Microfluidic protein crystallisation controlled using spontaneous emulsification

Microdroplet protein crystallization by utilizing spontaneous emulsification is reported. By utilizing this phenomenon, the crystal number control in a microdroplet was demonstrated. This method is expected to increase the flexibility of the protein crystallization screening system droplet microfluidics.

As featured in:



See Mao Fukuyama,
Akihide Hibara et al.,
Anal. Methods, 2015, 7, 7128.



Cite this: *Anal. Methods*, 2015, 7, 7128

Received 5th March 2015
Accepted 15th April 2015

DOI: 10.1039/c5ay00578g

www.rsc.org/methods

Microdroplet-based protein crystallisation using spontaneous emulsification is proposed and demonstrated. The dependence of water transport on the concentration of Span 80 was investigated. Crystallisation of the lysozyme was then demonstrated. Based on the results obtained, the dependency of the crystal number in a single microdroplet on the surfactant concentration was discussed.

Analysis of higher-order protein structures is essential for understanding their function in the fields of pharmacology, structural biology, and so on.¹ X-ray crystallography, in particular, is the most frequently used technique for the determination of higher-order structures and requires high quality protein crystals. To obtain high quality crystals, various experimental conditions, such as protein concentration, pH, temperature, a type of precipitant and its concentration, and the rate of protein condensation, require optimisation through numerous experiments.² The crystallisation process can therefore be a bottleneck for achieving high-throughput protein analysis.³

In recent years, the generation of microdroplets in microfluidic devices has received a great amount of attention as a platform for high-throughput screening of protein crystallisation conditions.^{4,5} In these microfluidic devices, monodispersed micrometre-sized droplets are generated individually on the millisecond time-scale.^{6,7} Microfabricated channel structures and well-defined flow conditions in the microfluidic devices enable precise control of the microdroplet size, the contents (e.g. solutes and cells) of the microdroplets, and both the outer and inner environments.^{8,9} In addition to the precise generation of microdroplets, a range of microdroplet manipulations,

including fusion,^{10,11} mixing,¹² storage,¹³ and *in situ* X-ray crystallography,^{14,15} have been reported. By utilising such technologies, both the concentrations and the species of the protein and the precipitant can be modified for each microdroplet. The screening of protein crystallisation conditions is therefore expected to be achieved with minimal sample amounts.

In microdroplet-based protein crystallisation, a batch method has been frequently applied, wherein supersaturated protein solutions are left under static conditions for a period of time.¹⁶⁻¹⁸ The use of microdroplets is preferable for nucleation number control, although nucleation with such a small volume requires a relatively long time, and so the applicability of the batch method for high-throughput screening is limited. In order to improve the applicability of microdroplet crystallisation for effective screening, the crystallisation probability can be modified by increasing the degree of supersaturation by the removal of water from the protein solution. Indeed, several condensation methods for aqueous microdroplets of protein solutions have already been proposed. Ismagilov *et al.*¹⁹ reported an alternative two-droplet configuration, where one droplet contains protein and the other contains a highly concentrated salt solution. Water present in the protein droplets is transported to areas of high salt concentration due to the osmotic pressure between the two droplets. Therefore, in this method, the rate of water transport was controlled by the distance between the droplets. Shim *et al.*²⁰ reported a poly(dimethylsiloxane) (PDMS) permeation method, where microdroplets of protein solution were trapped in PDMS chambers connected to a microchannel with a thin partition wall. In this method, a high concentration salt solution was flowed into the microchannel adjacent to the chambers. Water present in the microdroplets was then transported to the microchannel through the PDMS membrane, driven by osmotic pressure. In this case, the rate of water transport was controlled by the thickness of the wall. The rate of water transport in these studies was therefore optimised by the distance between the salt solution and the protein solution, which was controlled hydrodynamically or mechanically.

^aTokyo Institute of Technology, Ookayama, Meguro-ku, Tokyo 152-8551, Japan. E-mail: fukuyama.m.aa@m.titech.ac.jp; ahibara@chem.titech.ac.jp

^bKyoto Institute of Technology, Matsugasaki, Sakyo-ku, Kyoto 606-8585, Japan. E-mail: maofukuyama@kit.ac.jp

† Electronic supplementary information (ESI) available: (1) The cooling system; (2) calculation procedure of water flux; (3) the temporal variation of microdroplets of a protein solution; (4) explanation regarding the typical behaviours of the protein solutions. See DOI: [10.1039/c5ay00578g](https://doi.org/10.1039/c5ay00578g)



We herein report a simpler system to control the rate of water transport, based on nanodroplet formation by spontaneous emulsification. Spontaneous emulsification has been reported to occur in specific aqueous-organic-surfactant systems without a supply of external energy.²¹ We previously reported the selective concentration of microdroplet contents using spontaneous emulsification, induced by the non-ionic surfactant, Span 80.^{22,23} During the spontaneous emulsification in this system, the water molecules in microdroplets partition to a thin organic liquid membrane between the microdroplets and the nanodroplets, and partition to the nanodroplets. Water molecules are considered to transport by hydrating Span 80 molecules in the thin liquid membrane.²⁴ In the previous study, we found that the hydrophilic or large molecules were concentrated in microdroplets while the other molecules partitioned to nanodroplets generated from the microdroplets by spontaneous emulsification. Specifically, long fluorescein-tagged PEG (molecular weight of PEG part, $M_{\text{PEG}} = 2000$) was concentrated in the microdroplets while the short one ($M_{\text{PEG}} = 350$) partitioned to nanodroplets. In addition, protein (avidin) was almost quantitatively concentrated in the microdroplets. Our concept of protein crystallisation using spontaneous emulsification is shown in Fig. 1. When an aqueous microdroplet containing the protein and precipitant is exposed to an organic phase containing Span 80, nanodroplets form at the interface of the microdroplet. With nanodroplet formation, water is transported from the microdroplet to the nanodroplets, whilst the protein and the precipitant remain in the microdroplet. As a result, the concentration of the protein and precipitant increases, and a protein crystal forms. We therefore expected that using this method, the rate of water transport could be controlled by simply changing the surfactant concentration.

In this paper, we propose and demonstrate microdroplet-based protein crystallisation using spontaneous emulsification. Dependence of water transport on the concentration of Span 80 was investigated initially, followed by demonstration of the crystallisation of the protein lysozyme. Based on the results obtained, the control of the number of crystals formed in a single microdroplet is discussed.

In order to prepare the microdroplet array, a PDMS microfluidic device containing 100 microwells was used.²⁵ In this

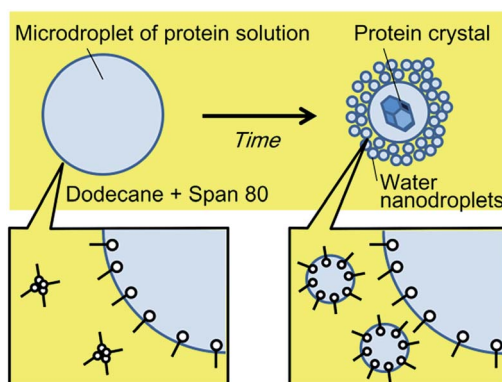


Fig. 1 Concept of microdroplet-based protein crystallisation using spontaneous emulsification.

device, 37 μm -deep square microwells with side lengths of 200 μm were prepared on the ceiling of a 50 μm -deep and 2 mm-wide straight channel. Fig. 2a illustrates the concept of the microdevice. Initially, an aqueous solution was introduced into each microwell, and each aqueous phase in the chamber was isolated by a flow of a dodecane (Wako Pure Chemicals, Japan) solution of Span 80 (Sigma-Aldrich KK, Japan) into the microchannel. The flow of the continuous (organic) phase was controlled at a rate of 5 $\mu\text{L min}^{-1}$ using a syringe pump (Model 100, BAS Inc. Japan). The micrographs of the microdroplets were obtained using a charge-coupled device (CCD) camera (Moticam 5.0, Shimadzu Co. Japan) with an interval of 5 min. As the volume of the aqueous solution in each microwell decreased, the array-filling aqueous solution (Fig. 2b) detached from the chamber wall, and was converted into a trapped droplet (Fig. 2c). For the protein crystallisation, a 120 mg mL^{-1} lysozyme solution (from egg white, Wako Pure Chemicals, Japan) containing 150 mM NaCl and 3 mM phosphate buffer (pH 6.0) was used. A Peltier cooling system was used to control the temperature of the solution. The dodecane solution of Span 80 (at room temperature (20 °C)) was introduced to the microdevice mounted on the cooling system set at -2 °C, and the temperature of the dodecane solution at the outlet was recorded as 1 °C.

The effect of Span 80 on the water transport rate was first investigated. Fig. 3a-d show the temporal variation of water microdroplets with a Span 80 concentration of 60 mM at room temperature. Initially, the microwells were filled with water, as shown in Fig. 3a. After several minutes, the water formed microdroplets (Fig. 3b). The initial droplet diameters were identical under all Span 80 concentration conditions (174–175 μm). These microdroplets then shrank, as a result of nanodroplet formation by spontaneous emulsification (Fig. 3c). In these experiments, the nanodroplets are generated at the interface of the microdroplet as previously reported,²² and the nanodroplets were removed by the organic flow right away. Finally, when the microdroplet shrank in size in comparison to the channel height, the microdroplets flowed away from the

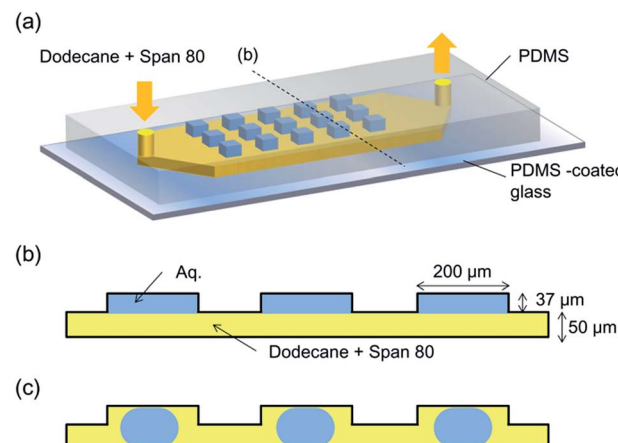


Fig. 2 A microfluidic device for microdroplet formation. (a) Overview of the device. A cross-sectional view of the microchannel shortly after the aqueous solutions were chambered (b), and when the solutions were exposed to a flow of dodecane containing Span 80 (c).



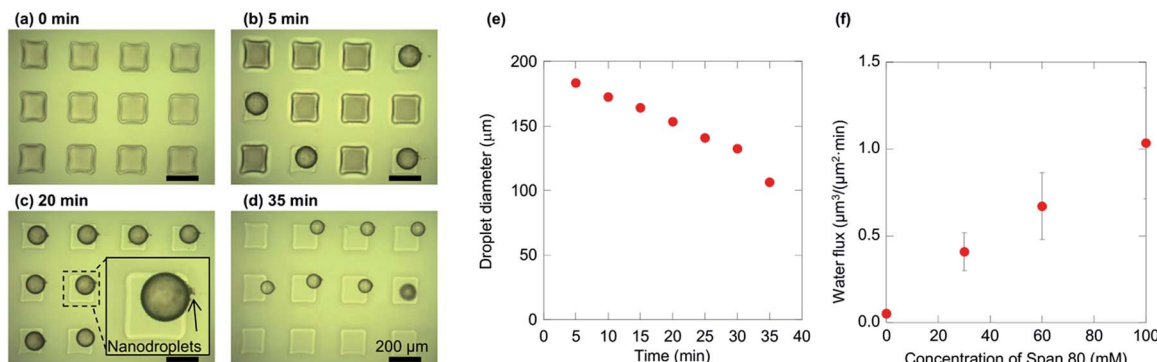


Fig. 3 Shrinkage of water microdroplets by spontaneous emulsification. (a)–(d) Micrographs of the droplets placed in the uppermost stream at 0, 5, 20, and 35 min using 60 mM Span 80. The continuous phase flowed from left to right. (e) The time-dependence of the diameter of the leftmost and middle droplets in (a)–(d). (f) The dependency of water flux from inside to outside the droplet, calculated from the micrographs (see ESI† for further details).

channels (Fig. 3d). Using a 60 mM Span 80 solution, the microdroplets were found to shrink from 180 μm to 100 μm within 35 min (Fig. 3e). The water flux from the inside to the outside of the microdroplets was calculated from the corresponding micrographs by assuming that the water flux was constant regardless of time based on the previous study²³ (see ESI† for details). The dependence of the water flux on the Span 80 concentration is shown in Fig. 3f, where it can be seen that the flux increased with Span 80 concentration. This observation is in agreement with previous laboratory-scale experiments, in which water transport from an aqueous to an organic phase containing a non-ionic surfactant was enhanced with an increase in its concentration.²⁶

The results indicated that the condensation factor of the microdroplet contents can be modified by the Span 80 concentration. When quantitative condensation is assumed, the condensation factor of the protein solution in a microdroplet is expressed as

$$R(t) = \frac{C(t)}{C_0} = \frac{V_0}{V(t)}, \quad (1)$$

where t , $R(t)$, $C(t)$, C_0 , $V(t)$, and V_0 indicate the time from microdroplet formation, condensation factor at t , protein concentrations at t and $t = 0$, volumes of microdroplet at t and $t = 0$, respectively. In the experiments, $V(t)$ can be expressed as the following recurrent equation;

$$V(t) = V_0 - \int_0^t S(V(t))Fdt, \quad (2)$$

where $S(V(t))$ and F indicate the interfacial area of a microdroplet at t and water flux, respectively. Here, $V(t)$ is a function of t , V_0 and F since $S(V(t))$ was determined by $V(t)$. Therefore, $R(t)$ was determined by F under the identical V_0 condition for all Span 80 concentrations.

Thus we considered that the protein crystal number in a microdroplet can be modified by the Span 80 concentration since the nucleation rate is known to be enhanced by a higher supersaturation degree.

Fig. 4 shows the micrographs of microwells filled with lysozyme solution after flowing through a solution of Span 80/dodecane for

130 min. In the absence of Span 80, no droplet formation was observed after subjecting the protein solutions to a flow of dodecane for 130 min (Fig. 4a), while in the presence of Span 80, water droplets formed (Fig. 3f). This may be due to the protein adsorption decreasing the hydrophobicity of the PDMS wall, thus preventing the dodecane solution from intruding between the protein solution and the walls of the microwells. In contrast, in the presence of a 100 mM solution of Span 80, the protein solutions partially or fully dissociated from the walls of the microwells, resulting in the formation of either microdroplets or sessile droplets (see ESI† for more details). Assuming that the height of the droplet was equivalent to the height of the well (*i.e.* 87 μm), the concentration factor of the protein solution was calculated to be 2. It was found that between 1 and 10 protein crystals were generated in each microdroplet, as can be seen in Fig. 4c, which shows a microdroplet containing 6 crystals. In contrast, Fig. 4d shows a droplet containing a single crystal (still growing) after flowing a dodecane solution containing 10 mM Span 80 for 180 min.

In Fig. 5, the distributions of the number of crystals in a droplet (N) in the presence of 0, 10, 30, and 100 mM Span 80 are shown. As expected, N was found to increase with increasing Span 80 concentration, as a high concentration induced a high nucleation frequency. This result indicates that the kinetics of protein crystallisation can be controlled by variation in the concentration of Span 80.

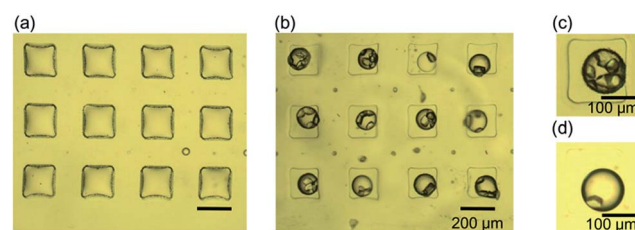


Fig. 4 Lysozyme crystallisation in microdroplets using spontaneous emulsification. Initial concentrations of lysozyme, NaCl, and phosphate buffer were 120 mg mL⁻¹, 150 mM, and 3 mM, respectively. Micrographs of the microwells after flowing dodecane solutions containing 0 mM (a) and 100 mM (b) Span 80 for 130 min. (c) and (d) Microdroplets containing 6 (c) and 1 (d) crystals.



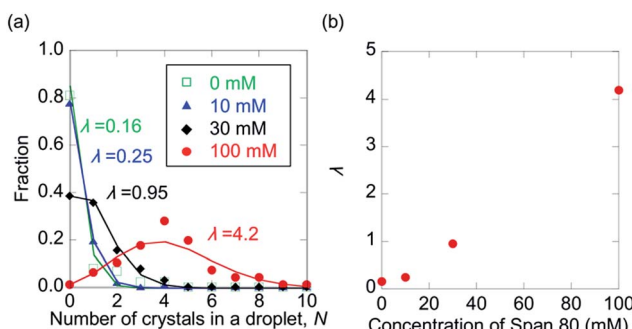


Fig. 5 The dependency of N on the concentration of Span 80. (a) The distributions of N using 0, 10, 30, and 100 mM Span 80. Lines indicate Poisson distributions with the expected values, λ , shown in the graph. (b) The dependency of λ on the concentration of Span 80.

In this method, the rate of water transport from the microdroplets of the protein solution can be controlled by varying the concentration of Span 80. Through this method, the water transport rate during protein crystal growth can be modified easily, a feat that is challenging in conventional vapour diffusion methods. A large crystal is therefore expected to be obtained by decreasing the crystal number in a microdroplet. This is achieved by decreasing the concentration of Span 80 after formation of the first nucleus. However, it should be noted that so far this method is not applicable to all the proteins because non-ionic surfactants, which interfere the crystallization of membrane proteins or protein complexes, have to be used. To solve this problem, the molecule structure of the surfactant should be optimized in the future. The dodecane dissolved in the microdroplets should also have some effect on the protein crystallization. In order to avoid this, the optimization of the continuous phase (e.g. usage of fluorous phase) should be investigated.

This method allows concentration of the protein solution by simply flowing a solution of Span 80 through the system, and does not require complex manipulations. This method is therefore expected to widen the feasibility of droplet crystallisation, which has wider implications not only for pharmaceutical applications, but also for fundamental studies of crystal growth.

Conclusion

Herein, we have reported for the first time, microdroplet protein crystallisation using spontaneous emulsification. The concentration of Span 80 was found to determine the rate of water transport from the microdroplets. By taking advantage of this phenomenon, crystal number control within microdroplets was demonstrated. This method is therefore expected to increase the flexibility of the protein crystallisation screening system.

Acknowledgements

Part of this work has been supported by KAKENHI (Grant-in-Aid for Challenging Exploratory Research 26620116, and for Scientific Research (A) 25248034). M.F. acknowledges Grant-in-Aid for JSPS Fellows.

Notes and references

- I. Tickle, A. Sharff, M. Vinkovic, J. Yon and H. Jhoti, *Chem. Soc. Rev.*, 2004, **33**, 558–565.
- A. McPherson, *Methods*, 2004, **34**, 254–265.
- N. E. Chayen, *Trends Biotechnol.*, 2002, **20**, 98.
- J. Leng and J.-B. Salmon, *Lab Chip*, 2009, **9**, 24–34.
- L. Li and R. F. Ismagilov, *Annu. Rev. Biophys.*, 2010, **39**, 139–158.
- S. Sugiura, M. Nakajima and M. Seki, *Langmuir*, 2002, **18**, 3854–3859.
- T. Thorsen, R. W. Roberts, F. H. Arnold and S. R. Quake, *Phys. Rev. Lett.*, 2001, **86**, 4163–4166.
- S. Y. Teh, R. Lin, L. H. Hung and A. P. Lee, *Lab Chip*, 2008, **8**, 198–220.
- G. F. Christopher and S. L. Anna, *J. Phys. D: Appl. Phys.*, 2007, **40**, R319–R336.
- W.-H. Tan and S. Takeuchi, *Lab Chip*, 2006, **6**, 757–763.
- N. Bremond, A. Thiam and J. Bibette, *Phys. Rev. Lett.*, 2008, **100**, 1–4.
- H. Song and R. F. Ismagilov, *J. Am. Chem. Soc.*, 2003, **125**, 14613–14619.
- C. H. J. Schmitz, A. C. Rowat, S. Köster and D. A. Weitz, *Lab Chip*, 2009, **9**, 44–49.
- K. Dhouib, C. K. Malek, W. Pfleider, B. G. Manuel, R. Duffait, G. Tuillier, R. Ferrigno, L. Jacquemet, J. Ohana, J. L. Ferrer, A. T. Dietrich, R. Giege, B. Lorber and C. Sauter, *Lab Chip*, 2009, **9**, 1412–1421.
- H. Yamaguchi, M. Maeki, K. Yamashita, H. Nakamura, M. Miyazaki and H. Maeda, *J. Biochem.*, 2013, **153**, 339–346.
- M. Maeki, Y. Teshima, S. Yoshizuka, H. Yamaguchi, K. Yamashita and M. Miyazaki, *Chem.-Eur. J.*, 2014, **20**, 1049–1056.
- W.-B. Du, M. Sun, S.-Q. Gu, Y. Zhu and Q. Fang, *Anal. Chem.*, 2010, **82**, 9941–9947.
- L. Li, D. Mustafi, Q. Fu, V. Tereshko, D. L. Chen, J. D. Tice and R. F. Ismagilov, *Proc. Natl. Acad. Sci. U. S. A.*, 2006, **103**, 19243–19248.
- B. Zheng, J. D. Tice, L. S. Roach and R. F. Ismagilov, *Angew. Chem., Int. Ed.*, 2004, **43**, 2508–2511.
- J.-U. Shim, G. Cristobal, D. R. Link, T. Thorsen, Y. Jia, K. Piattelli and S. Fraden, *J. Am. Chem. Soc.*, 2007, **129**, 8825–8835.
- C. López-Montilla, P. E. Herrera-Morales, S. Pandey and D. O. Shah, *J. Dispersion Sci. Technol.*, 2002, **23**, 219–268.
- M. Fukuyama and A. Hibara, *Proceeding of MicroTAS*, 2015, 224–226.
- M. Fukuyama and A. Hibara, *Anal. Chem.*, 2015, **87**, 3562–3565.
- L. Wen and K. D. Papadopoulos, *Colloids Surf. A*, 2000, **174**, 159–167.
- T. Wu, K. Hirata, H. Suzuki, R. Xiang, Z. Tang and T. Yomo, *Appl. Phys. Lett.*, 2012, **101**, 074108.
- N. Garti, S. Magdassi and D. Whitehill, *J. Colloid Interface Sci.*, 1985, **104**, 587.

